HUNGARIAN AGRICULTURAL ENGINEERING
No 43/2024 26-36
Published online: http://hae-journals.org/
HU ISSN 0864-7410 (Print)
HU ISSN 2415-9751(Online)
DOI: 10.17676/HAE.2024.43.26
Received: 10.05.2024 - Accepted: 05.07.2024

PERIODICAL
OF THE COMMITTEE OF AGRICULTURAL AND BIOSYSTEM ENGINEERING OF THE HUNGARIAN ACADEMY OF SCIENCES
and
HUNGARIAN UNIVERSITY OF AGRICULTURE AND LIFE SCIENCES
INSTITUTE OF TECHNOLOGY

OPTIMAL MATERIAL FLOW CHANNELS OF CROSS FLOW DRYERS

Author(s):
I. Keppler[1], A. Bablena[1]

Affiliation:
[1] Institute of Technology – Hungarian University of Agriculture and Life Sciences, 2100 Gödöllő, Páter Károly u. 1., Hungary;

Email address:
keppler.istvan@uni-mate.hu; bablena.adrienn@uni-mate.hu

Abstract: Reducing the moisture content of harvested grains is crucial for their subsequent processing or storage. Given the substantial energy requirements and potential environmental consequences associated with artificial drying, it is imperative to optimize the efficiency of this process. The quality of the final product is significantly impacted by inadequate or excessive drying, which is heavily influenced by the duration of grain exposure to the drying environment. Advances in dynamic modeling, facilitated by enhanced computational capabilities, have empowered researchers to intricately examine particle movement phenomena within drying equipment. In our study, we investigate variations in particle residence times under diverse geometric and tribological boundary conditions.

Keywords: granular materials, discrete element method, cross flow dryers, particle flow unevenness

1. Introduction

Reducing the moisture content of harvested grains is an essential part of preparing them for further processing or storage. Ideally, this task can be accomplished through natural drying, utilizing direct solar energy. However, the quantity of grains required to meet the food and raw material demands of developed industrial countries cannot be dried naturally; artificial drying is necessary. Due to the high energy demands and potential environmental impact of artificial drying, we must strive to perform the drying process with the highest possible efficiency.

2. The drying efficiency problem

In agriculture, drying can account for 60-80% of direct energy consumption [1], [2]. Therefore, it is evident that increasing drying efficiency is a fundamental interest for all enterprises involved in drying. There are two main directions for enhancing efficiency: optimizing thermodynamic processes (for example, by reducing the specific amount of fossil fuels used) and exploiting the potential opportunities in influencing particle movement processes.

In our article, we examine the second possibility. The development of explicit dynamic modeling methods, particularly the significant increase in computational capacity, has enabled researchers to study the particle movement processes occurring in drying equipment in detail [3], [4].

The quality of the final product is significantly affected by under-drying or over-drying, which is greatly influenced by the time the grain spends in the dryer [5]. The duration spent in the dryer depends on the velocity conditions of particle movement, which can be excellently analyzed using the discrete element method (DEM) [6].

To improve the efficiency of the drying process, we intend to investigate the following questions:

1. What dimensionless characteristic can be used to describe the uniformity of material flow within the dryer?

2. How do the tribological characteristics of interactions between particles and the wall affect the uniformity of material flow within the dryer?

3. How do the tribological characteristics of interactions between particles affect the uniformity of material flow within the dryer?
4. Is there a lamella geometry (different from straight) that can further improve the uniformity of material flow and thus enhance drying efficiency?

Theoretical considerations, experimental investigations and numerical simulations were conducted to achieve these objectives.

3. The Brachistochrone problem

The movement of grain in a dryer can be related to the solution of an ancient mathematical problem. The question of the downward motion of a particle sheds light on a classic problem in mechanics: the brachistochrone (shortest time) problem. This was first formulated by Johann Bernoulli [7], with the first solutions independently published by Newton and Leibniz [8], [9].

Bernoulli's question was as follows: What is the shape of the frictionless path along which a point mass will travel between two points, A and B, that are vertically aligned but not on the same vertical line, in the shortest possible time? (Figure 1.) This problem is one of the classic problems in the calculus of variations. The mathematical formulation of the problem is as follows [10]

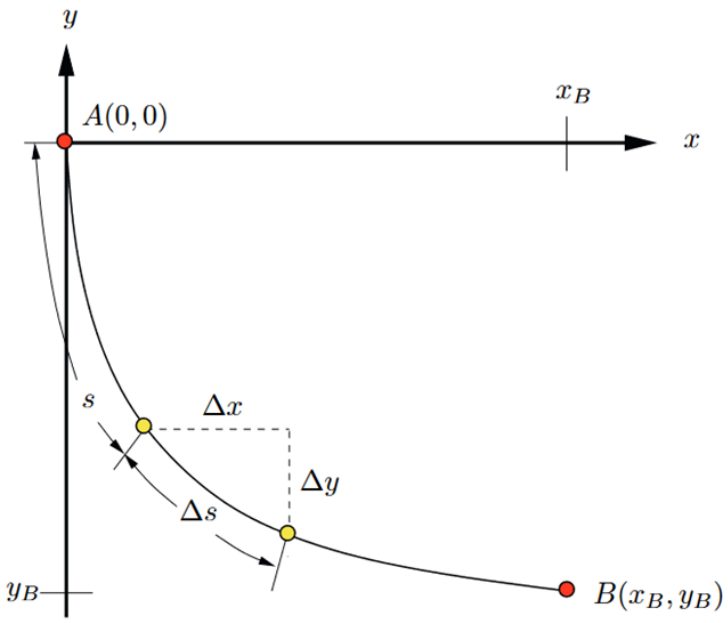

Figure 1. The Brachistochrone problem [11]

Time needed to move from *A* to *B*:

$$\int_A^B \frac{ds}{v} = \int_A^B \frac{ds}{\sqrt{2gy}}$$

Distance between points *A* and *B* is: $ds = \sqrt{x'(y)^2 + 1}dy$, so

$$t_{AB} = \frac{1}{\sqrt{2g}} \int_0^{y_B} \frac{\sqrt{x'(y)^2 + 1}}{\sqrt{y}} dy.$$

In this case, we seek the equation for the function $x(y)$ that minimizes the integral. To determine this, we write the Euler-Lagrange equation for the problem:

$$\frac{\partial f}{\partial x} = \frac{d}{dy}\frac{\partial f}{\partial x'}$$

where $f(x, x', y) = \frac{\sqrt{x'^2+1}}{\sqrt{y}}$. The solution of this differential equation is a cycloid:

$$x = a(\theta - \sin\theta)$$

$$y = a(1 - \cos\theta),$$

where parameter *a* is chosen according to the geometrical boundary conditions.

When considering friction, an analytical solution still exists, although it is significantly more complex. Numerous researchers have addressed this topic [12], [13], [14], [15], and the resulting curves differ only negligibly from the cycloid-shaped curve obtained in the frictionless case in practical applications [16]:

$$x(\theta) = \frac{C}{2}\left(\theta - \sin\theta + \mu\,(1 - \cos\theta)\right)$$

$$y(\theta) = \frac{C}{2}\left(1 - \cos\theta + \mu\,(\theta + \sin\theta)\right) + y_0,$$

where C and y_0 are chosen according to the geometrical boundary conditions.

Naturally, the motion of an entire granular assembly within a drying apparatus is a far more complex problem, as it requires considering interactions between the grains as well as between the grains and the walls. Therefore, we cannot expect an analytical solution to the proposed problem; instead, a numerical solution is necessary. The occasional interruption of material flow continuity precludes the use of finite element-based numerical methods, leading us to opt for the discrete element method.

4. Experimental investigations

Cross-flow drying equipment typically operates in a batch mode. During drying, the grain moves downward in a vertical direction, with deflector vanes ensuring that an adequate amount of air enters the equipment and that the grains remain in the dryer for the appropriate amount of time. We conducted particle movement experiments on both a large-scale industrial dryer and a model dryer. The obtained velocity values are shown on Figure 2.

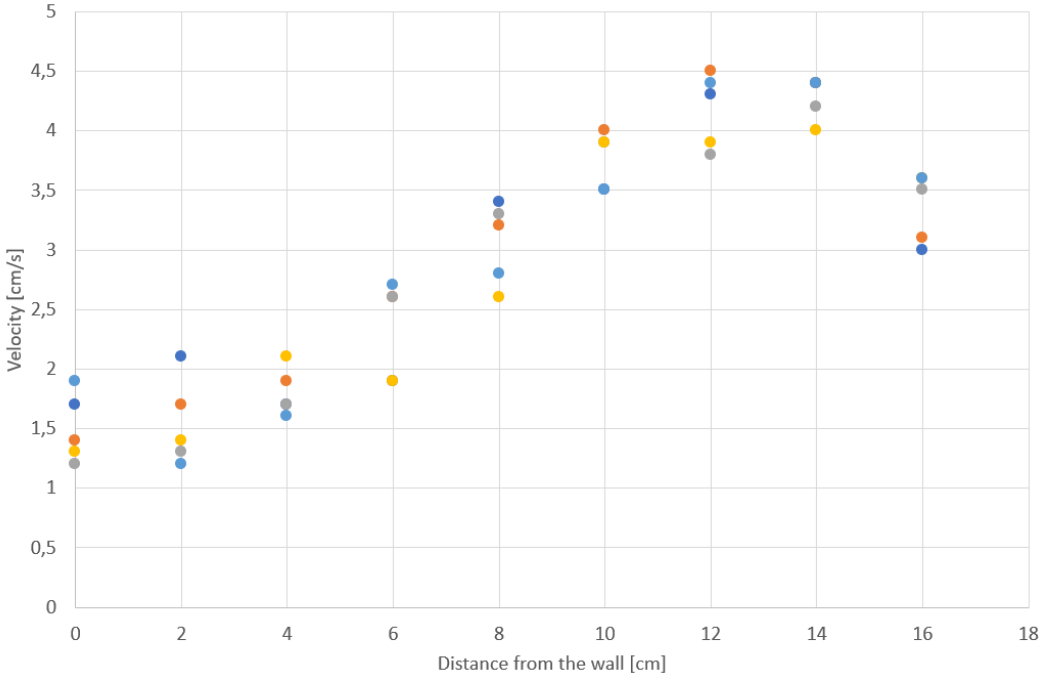

Figure 2. Velocity values measured around the lamella in the drying equipment

Figure 2. clearly shows that the presence of the lamellae significantly affects the flow velocity of the particles. A characteristic number that can describe the unevenness of the flow could be the

$$\vartheta = \frac{v_{\max} - v_{\min}}{v_{\max}}$$

quantity (velocity coefficient), which has a value of 0 for perfectly uniform flow, and approaches 1 as the unevenness increases. Based on the current measurement results, the average velocities corresponding to each distance value yield 0.65.

Particle movement studies were conducted both on the standalone drying module and inside the operational industrial drying equipment. Comparing the particle movement characteristics (velocity coefficients) between the standalone drying module and the operational industrial drying equipment, no significant differences in velocity coefficient values were observed.

Since measurements on the large dryer indicated that the vanes significantly influence the unevenness of particle flow, it was necessary to examine the effect of the vanes' inclination angle on velocity conditions. To facilitate this task, a model drying apparatus was constructed, consisting of two columns from the original drying module. The structure of the model dryer is depicted in Figure 3.

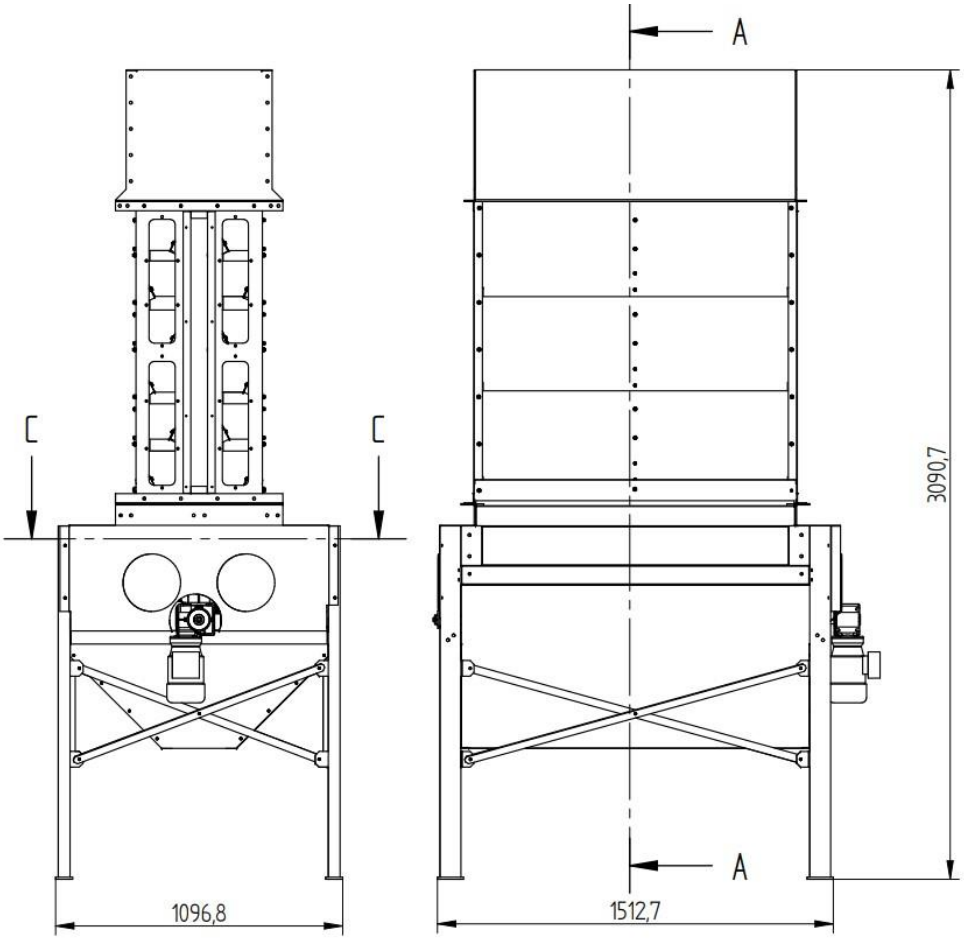

Figure 3. The model dryer apparatus

The flow velocity is primarily determined by the opening time of the discharge system. The rotational speed of the discharge unit in the model dryer was adjusted to generate velocity values that closely match those of the industrial dryer. We used painted layers to evaluate the particle displacements (Figure 4.).

Figure 4. Painted layers to analyze the particle displacement

As shown in Figure 5., good agreement in velocity ratios between the model dryer and the industrial drying equipment can be achieved by appropriately adjusting the opening time of the discharge unit.

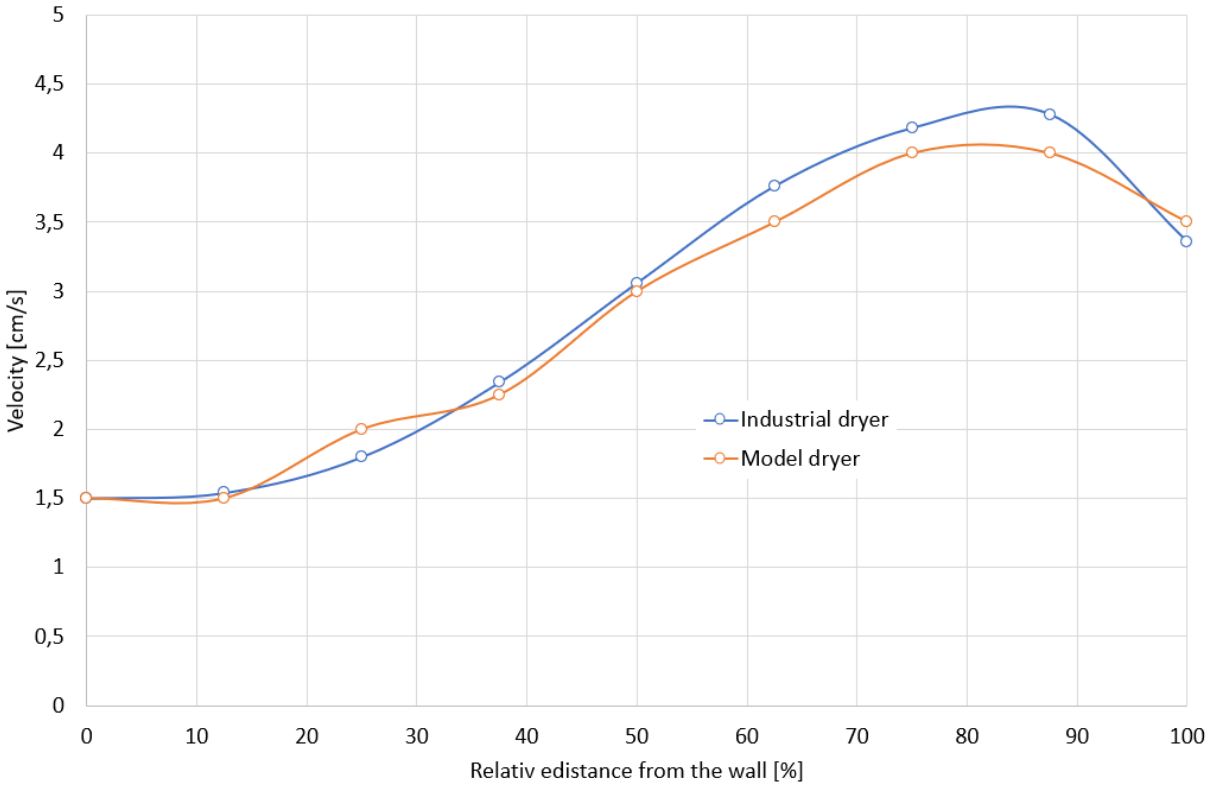

Figure 5. Comparison of the material flow conditions between the industrial and model dryers

5. The discrete element model

The discrete element method was developed by Cundall and Strack in the 1970s. When applying this method, the system solves the equations of motion for each individual particle in the assembly, taking into account the interactions between particles as well as between the particles and the bounding walls. To ensure adequate accuracy, calculations must be performed with very small time steps, making the method extremely computationally intensive for assemblies containing large quantities of particles [17].

To investigate the particle movements within the drying apparatus, we used the academic version of the EDEM 2.7 discrete element software. During the simulations, we consistently employed the "Hertz-Mindlin with no slip" contact model for calculating the contact forces between particles. The specified material characteristics and contact properties significantly influence the magnitudes of the normal and tangential force components. When using the mentioned contact model, the normal and tangential components of the forces can be calculated as follows:

$$F_n = \frac{4}{3}E_0\delta^{\frac{3}{2}}\sqrt{R_0} - 2\sqrt{\frac{5}{6}}\frac{\ln C_r}{\sqrt{\ln^2 C_r + \pi^2}}\sqrt{2E_0}\sqrt[4]{R_0\delta}\sqrt{m_0}v_{\text{nrel}},$$

$$F_t = -8G_0\sqrt{R_0\delta}\delta_t - 2\sqrt{\frac{5}{6}}\frac{\ln C_r}{\sqrt{\ln^2 C_r + \pi^2}}\sqrt{2G_0}\sqrt[4]{R_0\delta}\sqrt{m_0}v_{\text{trel}},$$

where $\frac{1}{E_0} = \frac{1-\nu_1^2}{E_1} + \frac{1-\nu_2^2}{E_2}$ gives us the reduced elastic modulus E_0. The normal overlap δ plays a significant role in the calculation of contact forces and can be determined as follows: consider two particles labeled i and j, with centers at positions x_i and x_j, and radii $R_i$and R_j. Then, $\delta = R_i + R_j - (x_j - x_i)$. The reduced radius in can be calculated as $R_0 = \frac{R_1R_2}{R_1+R_2}$, and the reduced mass is similarly calculated as $\mathrm{m}_0 = \frac{\mathrm{m}_1\mathrm{m}_2}{\mathrm{m}_1+\mathrm{m}_2}$. Finally, v_{nrel} represents the normal component of the relative velocity between the particles. $\frac{1}{G_0} = \frac{2-\nu_1}{G_1} + \frac{2-\nu_2}{G_2}$ and δ_t is the tangential deformation.

The normal F_n and tangential F_t force components between particles are related by Coulomb's law, such that $F_t = \mu_s F_n$, where μ_s is the coefficient of static friction. This relationship ensures that the tangential component cannot exceed the normal component.

In addition to the forces acting on the particles, the torque arising from these components can also be defined. The rolling torque M_r is given by $M_r = -\mu_r F_N R_i \omega_i$, where R_i denotes the distance between the centroid of particle *i* and the contact point, ω_i is the unit vector in the direction of the angular velocity vector, indicating the rotation direction of particle *i*, and μ_r is the coefficient of rolling friction. Similarly, the torque M_t due to the tangential force component F_t can be determined as $M_t = F_t R_i$.

During the simulations, the motion of each particle can be determined using the principles of linear and angular momentum. This defines a system of differential equations that can be solved numerically using many small time steps. The choice of the time step has a significant impact on the results and their accuracy. In my simulations, I used 25% of the Rayleigh time step (T_R) for the time increment (δt), that is:

$$\delta t = 0{,}25T_R = 0{,}25 \cdot (0.1631\nu + 0{,}8766)^{-1}\pi R\left(\frac{\rho_p}{G_p}\right)^{\frac{1}{2}}.$$

We have created the geometric model of the discharge opening and bottom lamellae (both straight and cycloidal case) of the drying apparatus (Figure 6.) for performing discrete element numerical simulations. The details of the model, boundary conditions, determination of micromechanical properties, and their values can be found in reference [18].

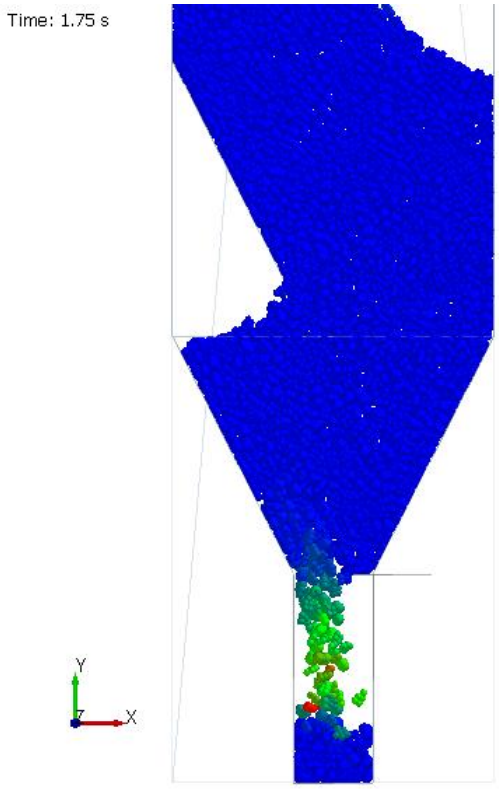

Figure 6. Discrete element model of the drying apparatus

Instead of studying velocity unevenness, in DEM investigations, we shifted our focus to examining the unevenness of the displacement field (Figure 7.):

$$\xi = \frac{y_{max} - y_{min}}{y_{max}}.$$

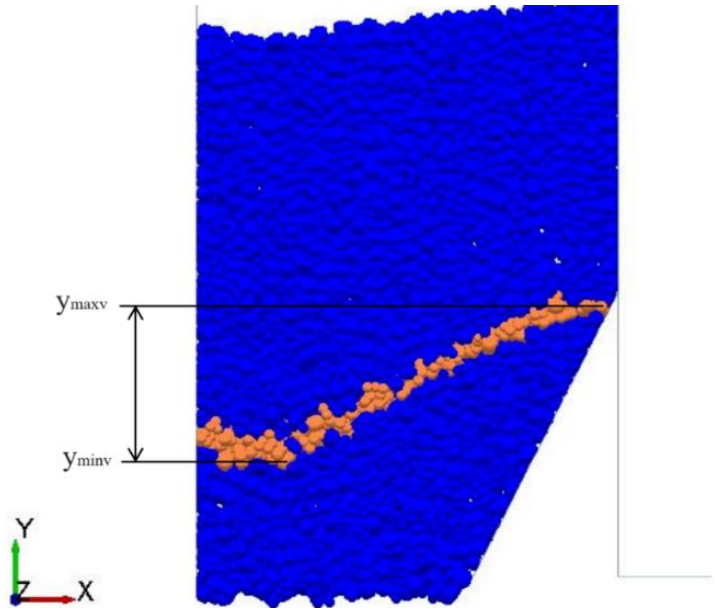

Figure 7. Determining flow unevenness from the displacement of particles

Based on analytical considerations in our earlier work, we demonstrated that cycloid-shaped vanes cause less flow unevenness.

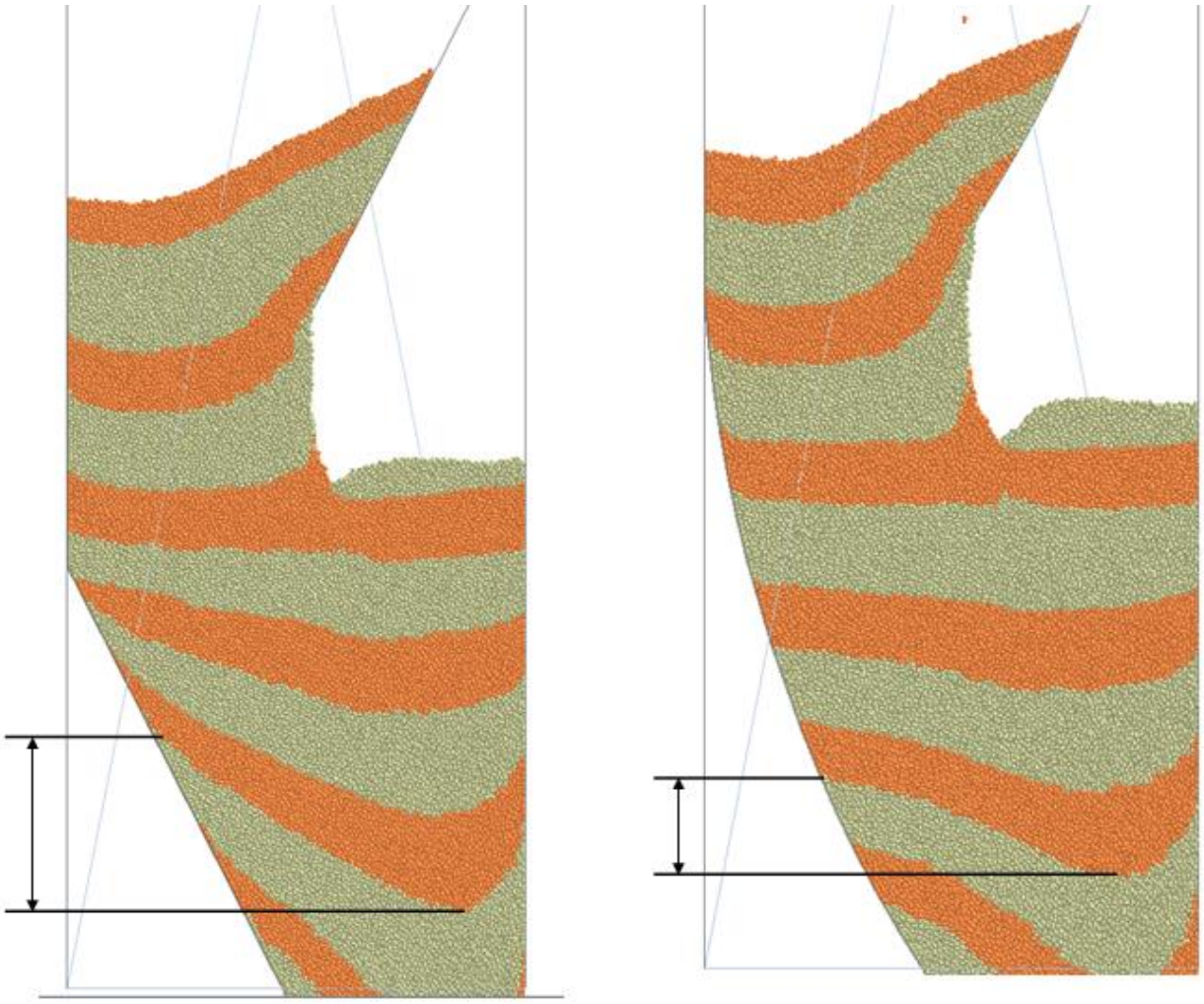

a., straight lamella *b.*, cycloidal lamella

Figure 8. Flow unevenness of different lamella geometries

Figure 8. shows a comparison of the uniformity of material flow. We can see the distortion of the originally horizontal striping after the same amount of time for both straight and cycloidal lamella cases. It can be observed that in the case of cycloidal lamella, this unevenness is much smaller. We also examined the value of flow unevenness for different particle-particle friction and wall friction values.

6. Results

To analyze the difference between the two types of lamella geometry, we introduced the flow unevenness difference as

$$\Delta = \frac{\xi_{straight} - \xi_{cycloidal}}{\xi_{straight}}.$$

As we can see on the following figures (Figure 9. and Figure 10.), the cycloidal lamella gives better results for all practically possible particle - wall and particle – particle friction values.

This result remarkably demonstrates that results developed through classical mechanical methods for the motion of a single particle remain applicable to some extent even when dealing with interactions among a large number of particles.

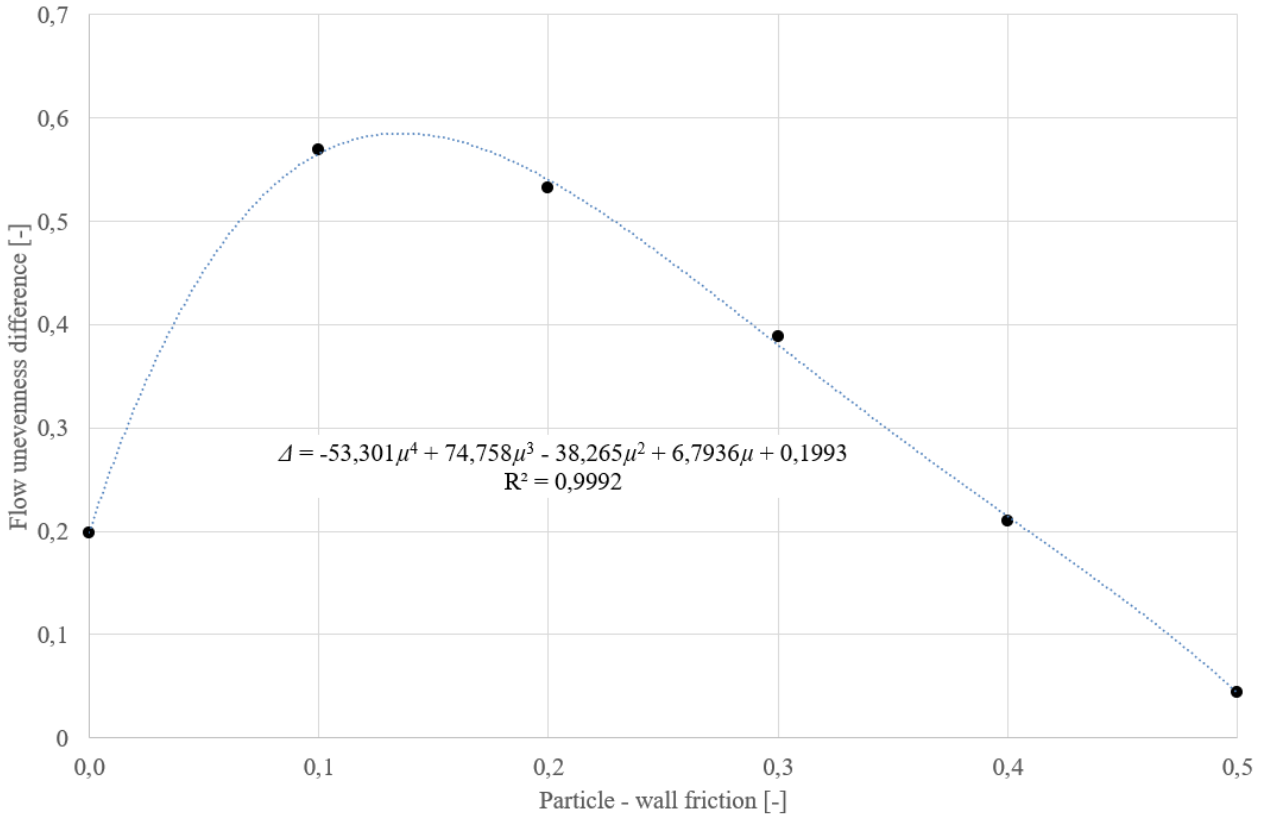

Figure 9. Flow unevenness difference as a function of particle – wall friction

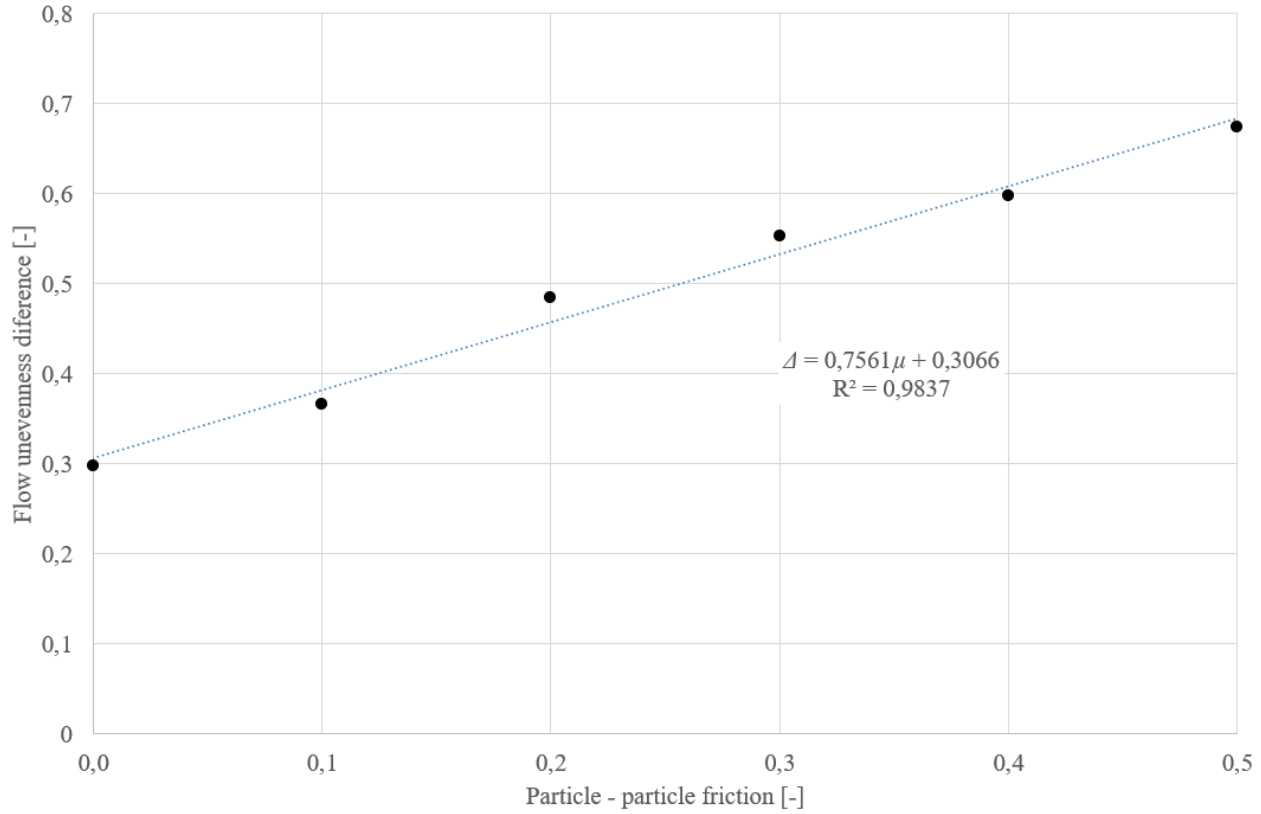

Figure 10. Flow unevenness difference as a function of particle – particle friction

From the above diagrams, we can see that the cycloidal-shaped lamella design ensures less flow velocity unevenness in all cases. Its effect on improving the flow pattern is particularly pronounced in cases of high internal friction (contamination).

7. Conclusions

To characterize the unevenness of material flow (by examining the movement of a designated strip in the material mass), we introduced the unevenness factor ξ. Using experimental investigations and numerical simulations, we demonstrated that the value of wall friction has a significant impact on the unevenness of material flow. Using experimental investigations and numerical simulations, we also demonstrated that the value of friction between particles has a significant impact on the unevenness of material flow. Using experimental investigations and numerical simulations, we showed that it is advisable to use cycloidal-shaped lamella in drying equipment. The cycloidal lamella resulted in a better unevenness factor for all particle-wall and particle-particle friction coefficient values we examined. To analyze the difference between the two types of lamella geometry, we introduced the flow unevenness difference. Its use enabled the quantitative determination of the results.

We found, that the flow unevenness difference as a function of particle-wall friction can be approximated with the polynomial equation

$$\Delta = -53.301\mu^4 + 74.758\mu^3 - 38.265\mu^2 + 6.7396\mu + 0{,}1993$$

within the interwall of particle – wall friction from 0 to 0.5. As the function of particle – particle friction we got a much simpler linear correlation:

$$\Delta = 0.7561\mu + 0{,}3066$$

within the interwall of particle – particle friction from 0 to 0.5.

Even though these two results provide an empirical formulation of the relationship between friction coefficients and the unevenness of material flow, they are surprisingly accurate in predicting the phenomenon. They can provide valuable insights into improving the understanding of the operational processes of drying equipment.

Acknowledgement

The authors appreciate the support of projects GINOP-2.1.2-8-1-4-16-2017-00285, GINOP-2.1.2-8.1.4-16-2017-00187 and GINOP-2.1.2-8-1-4-16-2017-00188.

References

[1] **Beke J.** (1997): Terményszárítás, Agroinform, Budapest, 419 p.
[2] **Baker, C.G.J.** (1997): Industrial Drying of Foods, Springer US, 978-0-7514-0384-8
[3] **Mellman, J., Teodorov, T.** (2011): Solids transport in mixed-flow dryers. Powder Technology, 205, 117-125. p.
[4] **Keppler, I., Kocsis, L., Oldal, I., Farkas, I., Csatár, A.** (2012): Grain velocity distribution in a mixed flow dryer. Advanced Powder Technology, 23, 824-832. p.
[5] **Mellman, J., Iroba, K.L., Meztger, T., Tsotas, E., Mészáros, Cs., Farkas, I.** (2011): Moisture content and residence time distributions in mixed-flow grain dryers. Biosystems Engineering, 109, 297-307. p.
[6] **Cundall, P.A. and Strack, O.D.L.** (1979) A discrete numerical model for granular assemblies. Geotechnique, 29(1), 47-65.
[7] **Bernoulli, J.** (1696): Problema novum ad cujus solutionem Mathematici invitatur. Acta Eruditorum, 18, 269 p.
[8] **Newton**, **I.** (1697): Philosophical Transactions of the Royal Society of London, 19, 424-425 p.
[9] **Leibnitz, G.W.** (1697): Acta Eruditorum, 19, 201-205 p.
[10] **Taylor, J.R.** (2005): Classical Mechanics. University Science Books, Colorado, 786 p.
[11] **Pesch H. J.** (2012): The Princess and Infinite-Dimensional Optimization Documenta Mathematica Extra Volume ISMP 345–356 p.

[12] **Wensrich, C.M.:** Evolutionary solutions to the brachistochrone problem with Coulomb friction. Mechanics Research Communications, 31, 151-159 p.
[13] **Hayen, J.C.** (2005): Brachistochrone with Coulomb friction. International Journal of Non-Linear Mechanics, 40, 1057-1075 p.
[14] **Čović, V., Vesković, M.** (2008): Brachistochrone on a surface with Coulomb friction. International Journal of Non-Linear Mechanics, 40, 437-450 P.
[15] **Sumbatov, A.S.** (2017): Brachistochrone with Coulomb friction as the solution of an isoperimetrical variational problem. International Journal of Non-Linear Mechanics, 88, 135-141 p.
[16] **Barsuk, A.A., Paladi, F.** (2023): On parametric representation of brachistochrone problem with Coulomb friction. International Journal of Non-Linear Mechanics, 148, 104265
[17] **Bagi, K.** (2007): A diszkrét elemek módszere, BME Tartószerkezetek Mechanikája Tanszék, Budapest, 73 p.
[18] **Keppler, I., Bablena, A**. (2024): Optimal lamella geometry for mixed flow dryers. Arch Appl Mech 94, 961–972.